Validation of Monte Carlo simulations by experimental measurements of neutron-induced activation in cyclotrons

Jonathan COLLIN[1,*], Jean-Michel HORODYNSKI[2], Nicolas ARBOR[1], Massimo BARBAGALLO[3], Federico CARMINATI[3], Giuliana GALLI CARMINATI[3], Luca J TAGLIAPIETRA[3] and Abdel-Mjid NOURREDDINE[1]

[1]Institut Pluridisciplinaire Hubert CURIEN (IPHC), CNRS, Université de Strasbourg, FRANCE
[2]ingénierie Radioprotection Sûreté Démantèlement (iRSD), CNRS, Université Paris-Saclay, FRANCE
[3]Transmutex SA, Suisse
(*) jonathan.collin@iphc.cnrs.fr

***Abstract*— Nuclear activation is the process of production of radionuclides by irradiation. This phenomenon concerns particle accelerators used in various fields, from medical applications to industrial ones, both during operation and at the decommissioning phase. For more than three decades, the possibility of using cyclotrons for nuclear power generation and nuclear waste reduction has also been discussed, i.e. in the case of Accelerator-Driven Systems [1]. The radioprotection and dismantling issues of accelerator facilities, that have been raised recently, is even more potent for such installations.**

In our study, we are particularly interested in the activation due to secondary neutrons produced by (x,n) reactions, mostly (p,n) occurring in the accelerator's components. This work focuses on the study of the radioactivity induced in various materials (V, Sc, Tb, W, Ta) irradiated by fast and thermal neutrons, in two different scenarios: through direct irradiation -with an AmBe source- and around an operating cyclotron at the CYRCé facility (Strasbourg). A broad Monte Carlo study including FLUKA, GEANT4, PHITS and MCNP simulation has been performed, with and without a FISPACT-II coupling, to estimate the reaction rates and to trace the induced radioactivity in samples of known composition. The results of the simulations are compared with the values extracted in two dedicated experimental campaigns in which activated samples underwent high resolution gamma-ray spectrometry.

Keywords **—Neutron activation, decommissioning, ADS, Fluka, PHITS, Geant4, FISPACT-II, MCNP6, HP-Ge spectrometry.**

I. INTRODUCTION

THE use of particle accelerators has expanded beyond the scientific field to include applications in the medical and industrial sectors, such as hadrontherapy and sterilization. The IAEA accounts for more than 577 accelerator facilities in the world [2], a number progressively increasing, in particular for particle therapy facilities, as seen on Figure 1.The dismantlement plans of such facilities were put on agenda at the beginning of XXIst century [3], but no related standards were established accordingly. Since then, the IAEA has been calling for stricter controls of the life-cycles of such facilities, with the idea to converge towards the standard of nuclear installations. The IAEA recommends the establishment of dismantling plans prior to any new commissioning of particle accelerator facilities. Such plans, that must be revised regularly (and at any upgrade or modifications to the facility), consists in a funding plan, an inventory of techniques and procedures for the decommissioning. The inventory of expected (and estimated) radionuclides produced during the life-cycle of facilities is of the utmost importance [4].

The relevance of such recommendations is more pertinent for the Accelerator Driven Systems (ADS) facilities, as they are both particle accelerator facilities and nuclear facilities. Indeed, ADS couples a nuclear reactor to a high-energy proton accelerator, allowing to produce energy as well as to transmute nuclear waste, in a safer subcritical regime [5]. Several ADS are currently being designed or constructed, such as the Transmutation Experimental Facility (TEF) (proton beam of 100 MeV -max 400 MeV/250 kW) [6], the Multipurpose Hybrid Research Reactor for High-tech Applications (MYRRHA) (600 MeV with 4 mA) [7], the Chinese Initiative Accelerator Driven Systems (CiADS) (250 MeV with 10 mA -max 1 GeV) [8] and the Subcritical Transmuting Accelerated Reactor Technology (START) from Transmutex (800 MeV with 5mA) [9].

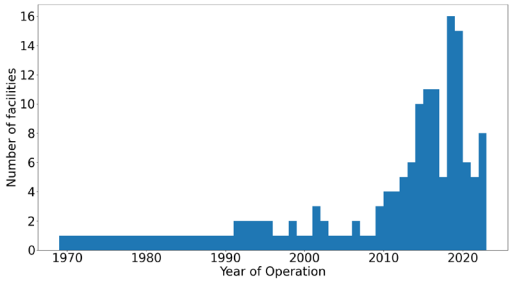

Figure 1 Particle therapy facilities in clinical operator since 1970 recorder by PTCOG *[10]*

The components of such systems will be activated by direct or indirect irradiation (secondary particles). Depending on the half-life of the radionuclides produced, an inventory is required for the radiation protection and the future dismantling plans. Hence the need for a quantitative radiological inventory, for which thermalized secondary neutrons are the main responsible for activation of components, primarily via (p,n) reactions [4], but (γ,n) reactions [11] and to some extent (α,n) reactions contribute as well to the inventory, in particular in the case of high energy cyclotrons, such the START system

Monte Carlo (MC) simulations of radiation-matter interactions are a powerful tool to estimate the induced activities and dose rates, as they can manage a great range of scenarios (fluence, irradiation/cooling time, …).

The objective of this work is to build a tool capable of accurately evaluate the radionuclides inventory for the START project. An exploration of which MC codes would be the most suitable for such application is necessary. This work is a first step to make an informed choice. We focused our development to activation studies for beam energy below 20 MeV, using the proton cyclotron CYRCé (Cyclotron for Research and Education) [12], available at the IPHC laboratory. This value corresponds, indeed, to physics models threshold in main Monte Carlo codes. The goal is to validate the methodology used here and apply it again to explore higher energy, where models may have greater discrepancies.

Neutron activation and (p,n) reactions will be discussed in this paper through the comparison of different MC codes, with an association to an analytical code (for activation computation). In the first section, the details on the codes used and the methodology adopted are reported, then the experimental setups (direct/indirect) and the codes used are presented. Finally, the simulation and the experimental results are compared.

II. Methodology

We will compare the four main MC tools for neutron capture and activation computation i.e., Fluka [13], [14], Geant4 [15], PHITS [16] and MCNP6 [17]. If most of them can do a radionuclides inventory natively, the access to an activity value is limited. Hence, the analytical code FISPACT-II [18] will be systematically used in association to the neutron spectra obtained via the mentioned MC tools. The comparison will be validated by experimental measurements, using high-resolution gamma spectrometry.

In 2020, the IAEA [4] suggested a list of materials, that are the most activated components in the accelerators environment, among them one can find iron, zinc, copper, aluminium, tungsten, steel, graphite, concrete, plastics, resins.

Using this list as a starting point, we selected V, Sc, Tb, Ta, W and Au samples to expose them to the two different types of neutron fields available. These samples were chosen according to the following criteria:

- Preferably only one stable nucleus.
- Materials available in foils and at high purity.
- Activation products half-life are compatible with gamma spectrometry and measures of radioprotection (access to irradiation zone, …)

Spectrometry using High Purity Germanium (HPGe) semiconductor detectors is one of the most widely used qualitative and quantitative multi-elemental analysis techniques in the field of radiation measurements. This technique allows the assessment of all γ-emitting radionuclides in a single analysis. The physical phenomena of radiation-matter interaction, for a given geometry, are integrated into a transfer function that provides the precise estimate of the sample's activity [19].

In this work, the measurements were performed with a HPGe LABSOCS from Canberra. The sensitivity of the setup used spans from 40 keV to 2650 keV with a relative efficiency of about 40%, while the resolution is 1.9 keV at 1.33 MeV. The system had been previously characterized using an ^{152}Eu source.

The activities were computed using the software Genie2000®, considering the decay scheme compiled by the Laboratoire National Henri Becquerel (LNHB) [20]. An example of measured spectra is provided Figure 3.

III. Experiments and Models

Two types of experiments have been performed, one with direct irradiation of neutron emitted by an AmBe source and another using the secondary neutron field produced by the interaction of the proton beam accelerated by the cyclotron and impinging on suited targets.

A. Direct neutron field

Two samples were irradiated with the AmBe source: Au and V. The isotropic ^{241}Am-Be neutron source used has an activity of 3.7×10^{10} Bq and a nominal neutron emission rate of 2.24×10^{6} n/s [21]. The AmO_2-Be powder is double-encapsulated within welded stainless-steel cylinders, which are inside of a Pb cylinder. The source was placed inside a paraffine (CH_2) barrel of 75 cm diameter and height, with 5 extruded cylinders, allowing to guide safely the source in the middle of the barrel, see Figure 2.

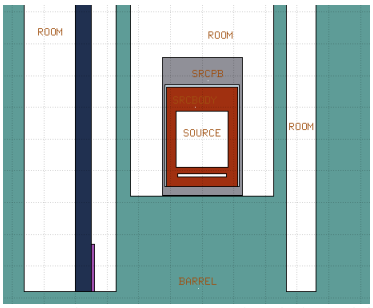

Figure 2. Am-Be experiment concept. Sectional view of the center of the paraffine barrel (teal) with PVC cane (dark blue) holding the sample (violet) close to the source (grey: lead shell, red: stainless steel)

The V (1.5x3x0.1cm^2) and Au (Ø1.2x0.1cm^2) samples were placed for respectively 32 and 6027 minutes inside the barrel and gamma spectrometry analysis were performed. One of the gamma spectra acquired is shown in Figure 3.

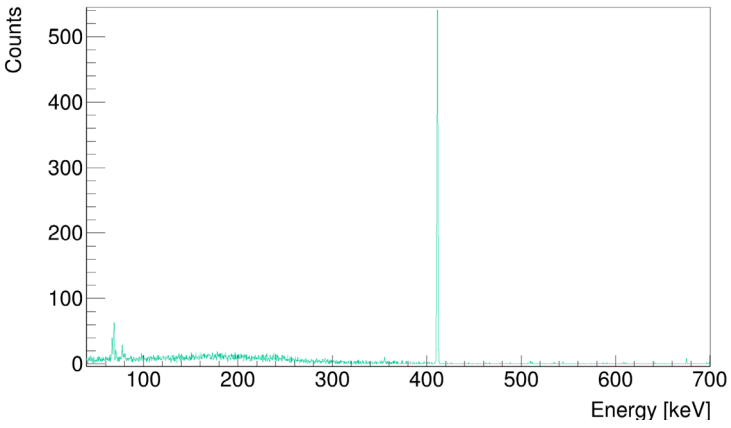

Figure 3. Gamma spectrometry of the Au sample irradiated using the AmBe neutron field measured by HP-Ge

B. Secondary neutron field

CYRCé is a TR24 from Advanced Cyclotron System Inc (ACSI), built in 2010 and installed in 2012. The experiment was conducted inside the cyclotron room, in the radioisotope line, which allows to produce ^{18}F, ^{89}Y and ^{64}Cu, with respectively a liquid target of enriched water (H_2O_{18}) and two solid targets (deposit of ^{89}Zr or ^{64}Ni). The targets are controlled by a selector that can align the devices with the beam. In this paper, only the secondary field from ^{18}F was studied.

Two runs were performed, using the 1 mL liquid target of enriched water (with 16.5 MeV primary protons), see

Table I and Table II for the detailed characteristics of the irradiations.

The standard dimensions of the samples, or activation detectors, are of 2.5x2.5 cm^2 and of thickness respectively 2 mm for Ta, 1 mm for Tb, 0.55 mm for Sc and 1 mm for Au. They were placed where high neutron flux was expected: inside the biological shield (where the target is located), on the biological shielding walls, next to the cyclotron yoke and on the wall in the periphery of CYRCé. The positions are shown in Figure 4.

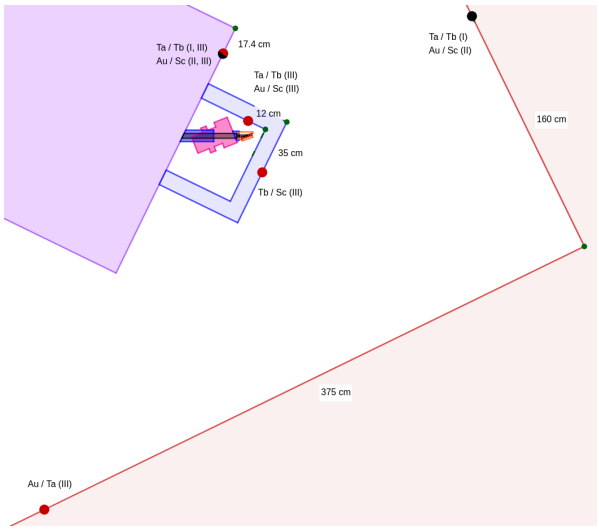

Figure 4. Historic of the locations for irradiated samples for the different runs (black dots for Run#1, red for the second one)

TABLE I
CHARACTERISTICS OF RUN#1

Primary beam	
Particle	Proton
Energy on target	16.5 MeV

Irradiation profile	
Irradiation [min]	Current [µA]
13	32
2880	0
23	34
1440	0
13	32
8640	0
14	30

TABLE II
CHARACTERISTICS OF RUN#2

Primary beam	
Particle	Proton
Energy on target	16.5 MeV

Irradiation profile	
Time length [min]	Current [µA]
17	35
1486	0
17	35
1354	0
19	35
8622	0
15	35

C. Model assumptions

1) Physics choices

To conduct this study, the options used for the MC tools will be detailed in the following:

- Fluka 2021.2.9

Neutrons are managed group-wise below 20 MeV (with 260 groups). ENDF/B-VIII.0 [22] cross-sections is used for all materials.

- FlukaCERN 4-3.2

In this case, the neutron point-wise cross-sections JEFF-3.3 library [23] is used for all materials.

- Geant4 11.0.3

The high precision models and cross-sections for neutron below 20 MeV is used (for elastic and inelastic scattering, capture and fission) through the physics lists ShieldingLEND [24] and QGSP_BIC_HP [25].

- PHITS 3.32

The photon transport EGS is activated. The library JENDL-4.0 [26] is used for neutron cross-sections.

- MCNP6.2

The neutron, proton and photon mode are activated in this simulation. The library ENDF/B-VII.1[27] were privileged. For the first irradiation run, TENDL-21 [28] neutron cross-section library was mainly used, excepted for ^{nat}C (ENDF/B-VII.1), ^{nat}Mg, ^{nat}S (ENDF/B-VI.8) and ^{nat}Si (ENDF/B-VI). TENDL-19 proton cross-section library is used for all materials instead of physics models excepted for H, ^{nat}C, ^{nat}Mg, ^{nat}S and ^{nat}Si.

- FISPACT-II

Is used in a two-step process, using the average neutron fluxes in the volume of interest. All computations were done with TENDL-19 library.

2) Geometrical choices

In the case of the direct irradiation, only the barrel and the surrounding air were modelled in the simulations. And for the AmBe, the ISO8529-1:2021 (small source) spectrum was assumed [29].

As far as the indirect irradiation is concerned, the concrete (Portland) walls, ground and floor close to the cyclotron were implemented, the cyclotron itself was simplified as a simple parallelepiped in stainless steel while a finer model was built for the target system components (target selector, target

support, …)

IV. Data and Analysis

The value of interest for these simulations were the incoming neutron spectra on the sample, as well as the production yield of nuclides inside the samples. This last value has been compared to experimental values acquired via gamma spectrometry and computed through FISPACT.

A. AmBe experiment

The neutrons produced by the Am-Be source are thermalised inside the paraffine barrel, maximizing the neutron capture rate in the vanadium and gold samples. The energy differential neutron flux calculated by various codes is reported in Figure 5. We found an agreement of all simulation for the energy spectrum of the neutron arriving on the sample, but for Geant4-ShieldingLEND which seems to have a different thermalisation behaviour. At thermal energy, the LEND (Low Energy Nuclear Data) model deviates of 43% from the MCNP value, when Fluka, PHITS and the High Precision (HP) from Geant4 stays below 8% of difference. For the fast neutron component, the standard deviation is within 5% for all models.

The four codes allow scoring the yield of the radioactive nuclei of interest. The simulation results are synthetised in the Table III. Fluka, PHITS and MCNP well agree within 1% (3% for Au). As for Geant4, while QGSP_BIC_HP stays within 3.9% (and 1% for Au), ShieldingLEND gives the most discrepancies with as much as 14% of difference for gold. We note that when using the physics list QGSP_BIC_HP the computation's speed is a factor 10 slower.

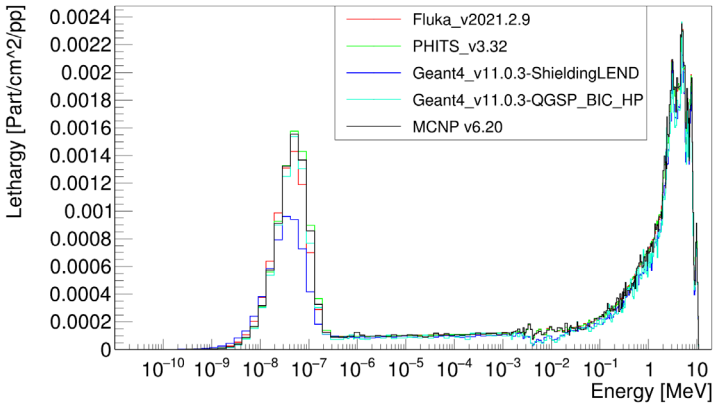

Figure 5. Track-length estimation of the neutron fluence inside the vanadium sample irradiated by the direct neutron field

Table III
COMPARISON OF EXPECTED YIELD IN THE IRRADIATED SAMPLES

Vanadium	
Code	Production rate [$\times 10^{-4}$ ^{52}V/pp]
Fluka	4.08 ± 0.002
Geant4 (ShieldingLEND)	3.78 ± 0.036
Geant4 (QGSP_BIC_HP)	4.24 ± 0.146
PHITS	4.05 ± 0.020

Gold	
Code	Production rate [$\times 10^{-3}$ ^{198}Au/pp]
Fluka	0.99 ± 0.002
Geant4 (ShieldingLEND)	0.87 ± 0.002
Geant4 (QGSP_BIC_HP)	1.02 ± 0.002
PHITS	1.02 ± 0.003

The same agreement has been found when considering FISPACT-II, as ashown in Figure 6. Native Fluka and Fluka coupled with FISPACT-II give same results within the given statistical uncertainties as well.

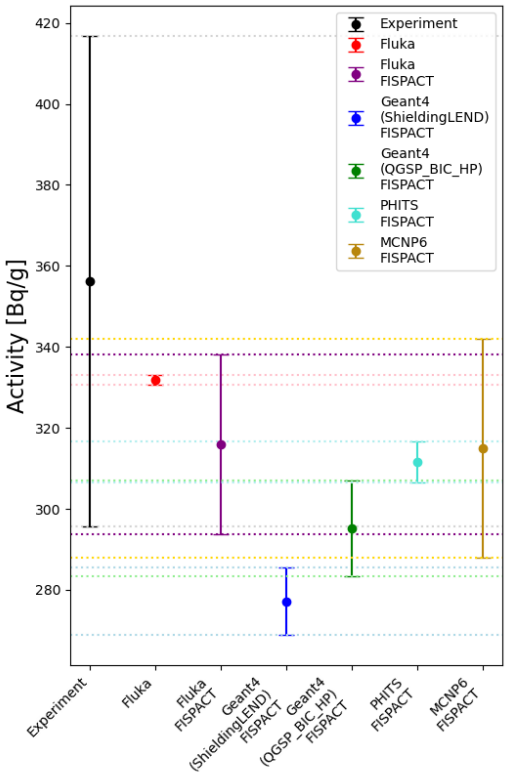

Figure 6. Compilation of measured vs estimated activities for the direct field experiment with the vanadium sample

Experimental data points were taken with V and Au, the samples were respectively activated at 357 ± 61 Bq/g and 318 ± 21 Bq/g. Considering uncertainties, the simulations are validated by the experimental data points.

B. CYRCé experiment

1) 1 mL target

Figure 7 shows the comparison between the activity value extracted using FLUKA-CERN one-step process and using FISPACT-II with fluence estimated with FLUKA-CERN (USRTRACK) and MCNP6.2 (f4). The measured values are also reported therein.

MCNP6/FISPACT-II results are in very good agreement with the experimental data. In most cases, FLUKA results are higher than experimental data, but large discrepancies seem to occur especially for Ta activation foils due to high uncertainties in the thermal neutron fluence range (Figure 8). Variance reductions techniques used with MCNP6 improve the statistics of the neutron fluence scored inside the activation foils (DXTRAN). Then, FLUKA-CERN model need to be improved to reduce statistical uncertainties without increasing the number of primary particles. Statistical uncertainties for neutron fluence estimated with FLUKA-CERN are larger than MCNP6 ones (Figure 8) although a higher number of primary particles than MCNP6 (7,4e7 for FLUKA-CERN, 4e7 for MCNP6) was used. Models and variance reduction set up in FLUKA-CERN model need to be improved to reduce statistical uncertainties without increasing the number of primary particles.

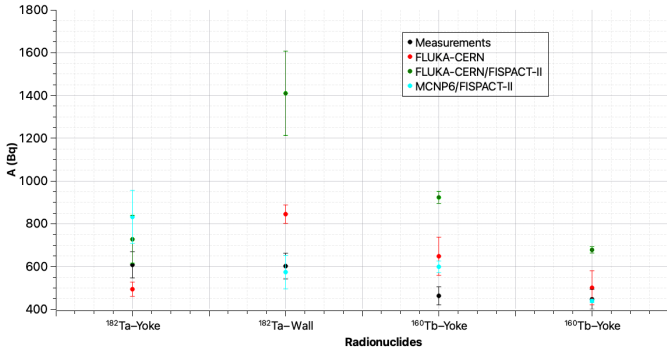

Figure 7. Activity comparison between measurements and estimated activities (indirect irradiation) using FISPACT-II, MCNP6 and FlukaCERN

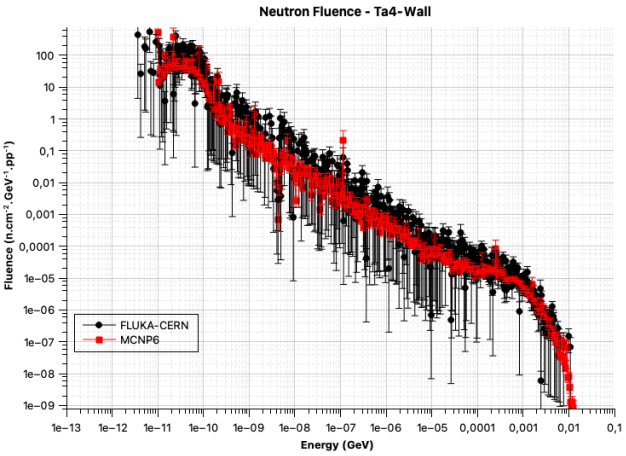

Figure 8. Neutron fluence for Ta foils located on the wall of the CYRCé bunker estimated with FLUKA-CERN and MCNP6

V. Conclusions and Perspectives

The objective of this work was to compare several MC codes, including a coupling with FISPACT, for two experimental scenarios: neutrons from AmBe source and secondary neutrons generated in a low energy cyclotron environment irradiated a set of samples and induced activations have been compared.

For the AmBe experiment, there is a good agreement between all the codes, and experimental values as well. While the Fluka, MCNP and PHITS agree within less than 3%, Geant4 and its ShieldingLEND physics list strays to 15%. This difference could be explained by a difference in the thermalisation process of neutron (Neutron managed with geant4 physics lists, not marked with '_HP' i.e., not with high precision models are not able to thermalise).

As for the irradiations at CYRCé cyclotron, MCNP6 code gives the best results, also thanks to the fact that the statistical uncertainties are reduced using efficient variance reduction techniques, especially for small regions like activation foils used in this study. FLUKA-CERN model needs to be improved to reduce statistical uncertainties for the neutron fluence. As for the experimental values, we plan increasing the concerned statistics as it is difficult to draw conclusions with the current uncertainties.

If one can compare codes through the yield of nuclei per primary atoms, to confront to experimental value with ease, FISPACT-II remains essential. As well as for the intercomparison of codes, this analytical allows to compare radionuclides inventories with the neutron spectra as the only input, restraining the number of influences.

To further the study, the irradiation campaign is ongoing, and it features other kinds of target (liquid and solid) and new locations for activation foils. Comparisons will be made with Solid-State nuclear track detectors. Geant4 and PHITS code will be included in the panel of MC code in the cyclotron studies.

Transmutex is also developing its own MC tool, called TMX-MC, based on Geant4 to simulate its nuclear and particle accelerator installation, as well as the dismantling of the last one. This code will join the panel of MC tools compared, for radiological inventories and radiation protection studies.

To extend this work, we are planning a systematic intercomparison of codes, in particular for neutron capture in the full range from thermal neutrons to ultrafast. A complete survey of (x,n) reactions of interest in proton accelerators up to GeV will also be carried out to address the problem of ADS decommissioning.

Acknowledgment

The authors would like to thank the CYRCé technical team and in particular M. PELLICIOLI, as well as T. FOEHRENBACHER for the spectrometry measurements.

References

[1] C. Rubbia *et al.*, "Conceptual design of a fast neutron operated high power energy amplifier", *CERN*, 1995.

[2] "Cyclotron Master List - cyclotrons_view_2020", Jun. 08, 2023. https://nucleus.iaea.org/sites/accelerators/lists/cyclotron%20master%20list/cyclotrons_view_2020.aspx#InplviewHashb4c61c57-92e3-4919-885c-7bc3bba78de7=Paged%3DTRUE-p_ID%3D271-PageFirstRow%3D151 (accessed Jun. 08, 2023).

[3] Université libre de Bruxelles, Ed., *Evaluation of the radiological and economic consequences of decommissioning particle accelerators: final report*. in EUR Nuclear safety and the environment, no. 19151. Luxembourg: Off. for Off. Publ. of the European Communities, 1999.

[4] I. A. E. Agency, "Decommissioning of Particle Accelerators", International Atomic Energy Agency, Text, 2020. Accessed: Jun. 02, 2023. [Online]. Available: https://www.iaea.org/publications/12371/decommissioning-of-particle-accelerators

[5] H. Nifenecker, S. David, J. M. Loiseaux, and O. Meplan, "Basics of accelerator driven subcritical reactors", *Nucl. Instrum. Methods Phys. Res. Sect. Accel. Spectrometers Detect. Assoc. Equip.*, vol. 463, no. 3, pp. 428–467, May 2001, doi: 10.1016/S0168-9002(01)00160-7.

[6] T. Sasa, "Design of J-PARC Transmutation Experimental Facility", *Prog. Nucl. Energy*, vol. 82, pp. 64–68, Jul. 2015, doi: 10.1016/j.pnucene.2014.07.031.

[7] "MYRRHA: Preliminary front-end engineering design - ScienceDirect". https://www-sciencedirect-com.scd-rproxy.u-strasbg.fr/science/article/pii/S036031991500717X (accessed Aug. 01, 2023).

[8] Z. Wang *et al.*, "Materials for Components in Accelerator-driven Subcritical System", *Strateg. Study Chin. Acad. Eng.*, vol. 21, no. 1, Art. no. 1, doi: 10.15302/J-SSCAE-2019.01.006.

[9] "TECHNOLOGY | Transmutex_technology", *Transmutex*. https://www.transmutex.com/technology (accessed Aug. 01, 2023).

[10] "PTCOG - Facilities in Operation". https://ptcog.site/index.php/facilities-in-operation-public (accessed Aug. 01, 2023).

[11] S. Hu, K. Fan, L. Zhang, Z. Mei, X. Li, and Z. Zeng, "Beam loss issue study on the extraction system of a superconducting cyclotron

at HUST", *Nucl. Instrum. Methods Phys. Res. Sect. Accel. Spectrometers Detect. Assoc. Equip.*, vol. 911, pp. 87–93, Dec. 2018, doi: 10.1016/j.nima.2018.09.126.

[12] E. Bouquerel *et al.*, "Design and commissioning of the first two CYRCé extension beamlines", *Nucl. Instrum. Methods Phys. Res. Sect. Accel. Spectrometers Detect. Assoc. Equip.*, vol. 1024, p. 166034, Feb. 2022, doi: 10.1016/j.nima.2021.166034.

[13] A. Ferrari, P. R. Sala, A. Fasso, and J. Ranft, "FLUKA: A Multi-Particle Transport Code", SLAC-R-773, 877507, Dec. 2005. doi: 10.2172/877507.

[14] T. T. Böhlen *et al.*, "The FLUKA Code: Developments and Challenges for High Energy and Medical Applications", *Nucl. Data Sheets*, vol. 120, pp. 211–214, Jun. 2014, doi: 10.1016/j.nds.2014.07.049.

[15] J. Allison *et al.*, "Recent developments in Geant4", *Nucl. Instrum. Methods Phys. Res. Sect. Accel. Spectrometers Detect. Assoc. Equip.*, vol. 835, pp. 186–225, Nov. 2016, doi: 10.1016/j.nima.2016.06.125.

[16] T. Sato *et al.*, "Features of Particle and Heavy Ion Transport code System (PHITS) version 3.02", *J. Nucl. Sci. Technol.*, vol. 55, no. 6, pp. 684–690, Jun. 2018, doi: 10.1080/00223131.2017.1419890.

[17] C. J. Werner *et al.*, "MCNP Version 6.2 Release Notes", Los Alamos National Lab. (LANL), Los Alamos, NM (United States), LA-UR-18-20808, Feb. 2018. doi: 10.2172/1419730.

[18] J.-Ch. Sublet, J. W. Eastwood, J. G. Morgan, M. R. Gilbert, M. Fleming, and W. Arter, "FISPACT-II: An Advanced Simulation System for Activation, Transmutation and Material Modelling", *Nucl. Data Sheets*, vol. 139, pp. 77–137, Jan. 2017, doi: 10.1016/j.nds.2017.01.002.

[19] ISO20042, "Measurement of radioactivity - Gamma-ray emitting radionuclides - Generic test method using gamma-ray spectrometry", Aug. 2021.

[20] "Nucléide – Lara Application – Laboratoire National Henri Becquerel". http://www.lnhb.fr/nuclear-data/module-lara/ (accessed Aug. 02, 2023).

[21] K. Amgarou *et al.*, "Characterization of the neutron field from the 241Am-Be isotopic source of the IPHC irradiator", *Radiat. Meas.*, vol. 50, pp. 61–66, Mar. 2013, doi: 10.1016/j.radmeas.2012.11.015.

[22] D. A. Brown *et al.*, "ENDF/B-VIII.0: The 8th Major Release of the Nuclear Reaction Data Library with CIELO-project Cross Sections, New Standards and Thermal Scattering Data", *Nucl. Data Sheets*, vol. 148, pp. 1–142, Feb. 2018, doi: 10.1016/j.nds.2018.02.001.

[23] A. J. M. Plompen *et al.*, "The joint evaluated fission and fusion nuclear data library, JEFF-3.3", *Eur. Phys. J. A*, vol. 56, no. 7, p. 181, Jul. 2020, doi: 10.1140/epja/s10050-020-00141-9.

[24] "Shielding — PhysicsListGuide 11.1 documentation". https://geant4-userdoc.web.cern.ch/UsersGuides/PhysicsListGuide/html/reference_PL/Shielding.html#shielding (accessed Aug. 10, 2023).

[25] "QGSP_BIC — PhysicsListGuide 11.1 documentation". https://geant4-userdoc.web.cern.ch/UsersGuides/PhysicsListGuide/html/reference_PL/QGSP_BIC.html#qgsp-bic (accessed Aug. 10, 2023).

[26] K. SHIBATA *et al.*, "JENDL-4.0: A New Library for Nuclear Science and Engineering", *J. Nucl. Sci. Technol.*, vol. 48, no. 1, pp. 1–30, Jan. 2011, doi: 10.1080/18811248.2011.9711675.

[27] M. B. Chadwick *et al.*, "ENDF/B-VII.1 Nuclear Data for Science and Technology: Cross Sections, Covariances, Fission Product Yields and Decay Data", *Nucl. Data Sheets*, vol. 112, no. 12, pp. 2887–2996, Dec. 2011, doi: 10.1016/j.nds.2011.11.002.

[28] A. J. Koning, D. Rochman, J.-Ch. Sublet, N. Dzysiuk, M. Fleming, and S. van der Marck, "TENDL: Complete Nuclear Data Library for Innovative Nuclear Science and Technology", *Nucl. Data Sheets*, vol. 155, pp. 1–55, Jan. 2019, doi: 10.1016/j.nds.2019.01.002.

[29] ISO8529-1, "Neutron reference radiations fields - Part 1 : characteristics and methods of production", Dec. 2021.